Reactive & Functional Polymers 70 (2010) 223–229

Contents lists available at ScienceDirect

Reactive & Functional Polymers

journal homepage: www.elsevier.com/locate/react

Synthesis of a polyoxadiazole containing the 4-hydroxypyridine group and photo-induced fluorescent imaging on the polymer film

Young-shin Kim [a,b], Dai Geun Kim [c], Na Young Kwon [a], Hyung Jun Kim [a,d], Moon Soo Choi [a,e], Minjung Lee [f], Taek Seung Lee [g,*]

[a] Organic and Optoelectronic Materials Laboratory, Department of Advanced Organic Materials and Textile System Engineering, Chungnam National University, Daejeon 305-764, Republic of Korea
[b] Aekyung ChemTech Co., Ltd., R&D Center, 217-2, Shinseong-dong, Yuseong-gu, Daejeon 305-345, Republic of Korea
[c] Organic and Optoelectronic Materials Laboratory, Department of Nanotechnology, Chungnam National University, Daejeon 305-764, Republic of Korea
[d] Hyosung Corporation, 183-2 Hoge-dong, Dongan-gu, Anyang, Gyeonggi-do 431-080, Republic of Korea
[e] Display Materials R&D Center, Samsung Cheil Industries Inc., 332-2 Gocheon-dong, Uiwang, Gyeonggi-do 437-711, Republic of Korea
[f] Department of Oriental Medicine and Food Biotechnology, Joongbu University, 101 Daehack-ro, Chubu-myon, Kumsan-gun, Chungnam 312-702, Republic of Korea
[g] Organic and Optoelectronic Materials Laboratory, Department of Advanced Organic Materials and Textile System Engineering and Graduate School of Analytical Science and Technology (GRAST), Chungnam National University, Daejeon 305-764, Republic of Korea

ARTICLE INFO

Article history:
Received 12 October 2009
Received in revised form 9 December 2009
Accepted 9 December 2009
Available online 16 December 2009

Keywords:
Conjugated polymers
Polyoxadiazole
Fluorescence
Fluorescent imaging

ABSTRACT

A polyoxadiazole containing the 4-hydroxypyridine group, introduced to enhance the intermolecular interaction between polymer chains as well as for photosensitization, was synthesized from a corresponding precursor polyhydrazide. The absorption and emission spectra of the polymer film exhibited red-shifted maxima compared to those of the polyoxadiazole in chloroform solution, indicative of the presence of significant intermolecular interactions. The synthesized polymer showed a unique fluorescence enhancement upon UV irradiation in solution as well as in the film, presumably due to the photosensitized oxidation of hydroxypyridine groups to produce pyridone structures having different intermolecular interactions. Thus, this phenomenon enabled us to obtain a stable patterned image with enhanced fluorescence intensity in the UV-exposed area of the polymer film without any subsequent processes such as baking or etching.

1. Introduction

In the past decades, conjugated polymers with extended π-conjugation have received a great deal of attention [1,2] because of their unique properties such as electrical conductivity [3], electroluminescence [4], and chemical sensing [5], which have potential applications in devices such as light-emitting diodes, photovoltaic cells, and thin-film transistors [6,7]. A number of conjugated polymers with various kinds of structures have been synthesized to introduce functional groups into the conjugated backbone not only to change the luminescent properties but also to endow the polymers with new functions [8].

Among these, π-conjugated polymers with nitrogen-containing fused-ring structures are one of the most promising categories of fluorescent polymers because of their high fluorescence, high electron mobility, and easy tailoring of their chemical structure [9–11]. Aromatic oxadiazole-based compounds have an electron-withdrawing imine nitrogen (C=N) framework and have attracted interest because they have a high electron affinity, which facilitates both electron injection and transport, as well as excellent mechanical, thermal, and thermo-oxidative stabilities [12,13]. Thus, polymers containing an oxadiazole moiety have been widely used in electronic devices such as electron-transporting materials because the presence of the oxadiazole ring in the molecular backbone affects the electronic properties of the resulting polymers [14–18].

A number of studies on fluorescence-controlled organic systems have been undertaken to develop optical data storage [19,20]. Systems consisting of tert-butoxycarbonyl (t-Boc)-protected quinizarin or coumarin moieties with a photoacid generator (PAG) are one of the more prominent examples [21,22]. Most of the current-generation methods for the production of fluorescent patterned images in polymer films are closely connected to photo-induced chemical transformations of substrates in exposed areas of polymer films in the presence of PAG with the subsequent formation of ionic or hydrogen-bonding interactions between newly formed reactive groups and functional dyes. This procedure has potential limitations such as the essential requirement for PAG, the

* Corresponding author. Tel.: +82 42 821 6615; fax: +82 42 823 3736.
E-mail address: tslee@cnu.kr (T.S. Lee).

1381-5148/$ - see front matter © 2009 Elsevier Ltd. All rights reserved.
doi:10.1016/j.reactfunctpolym.2009.12.003

long-term instability of patterned images due to the presence of residual PAG, and the need for subsequent steps such as baking or etching. As described elsewhere, photolytic or thermolytic byproducts as well as PAG remaining in the film after image patterning can reduce the image resolution and deteriorate the long-term stability of the patterned image [23]. Thus, photodegradation-induced fluorescence imaging in the absence of PAG has been reported [24].

Recently, we demonstrated a fabrication method for a patterned image on a flexible substrate such as flexible electrospun fiber mats [25,26] as well as on silicon wafers [27]. We also demonstrated simple and effective fluorescent imaging on a hydroxyphenylbenzoxazole polymer film by means of UV irradiation without the aid of PAG and post-processing [28]. The key mechanism of such patterning is related to the manipulation of intermolecular π-interaction between hydroxyphenylbenzoxazole groups in the backbones by UV irradiation.

In this work, we report a simple method for synthesizing a conjugated oxadiazole with hydroxypyridine groups in the main chain and for fabricating fluorescent images in the resulting polymer films in the absence of PAG. It is well-known that the hydroxypyridine chromophore is a component of the sensitizer used for photooxidation to produce pyridine-4(1H)-one during photoirradiation [29–31]. We conjectured that the presence of hydroxypyridine groups in the polymer chain would enable the formation of intermolecular hydrogen bonds between polymer chains. Upon irradiation, it was expected that the hydroxypyridine moieties would be converted into pyridone groups, which would lessen the intermolecular interaction between chains. Accordingly, we expected that the polymer would show a unique fluorescence property in solution and in film form upon UV illumination, allowing for easy and simple fluorescent imaging. To our knowledge, this is the first report of this type of simple fluorescent pattern imaging using the unique phenomenon of fluorescence-intensity enhancement without the aid of PAG.

2. Experimental

2.1. Materials and reagents

All the chemicals and reagents were purchased from Aldrich and used without further purification unless otherwise specifically noted. 2,5-Dihydroxyterephthalic acid, 1-bromohexadecane, 2-ethylhexyl bromide, and chelidamic acid were purchased from Aldrich and used as received.

2.2. Characterization

^{1}H and ^{13}C NMR spectra were collected on a Bruker DRX-300 spectrometer, with tetramethylsilane as an internal standard (Korea Basic Science Institute). UV–Vis absorption spectra were recorded on a PerkinElmer Lambda 35 spectrometer. Luminescence spectra were collected on a PerkinElmer LS 45 spectrometer, with a xenon lamp as a light source. The molecular weight was determined by gel-permeation chromatography (GPC), with tetrahydrofuran (THF) as an eluent with a polystyrene standard. The elemental analysis was determined with a CE Instruments EA-1110 elemental analyzer. Differential scanning calorimetry (DSC) was performed on a DuPont model 2100 thermal analyzer equipped with a 2910 DSC instrument at a heating rate of 10 °C/min under a nitrogen atmosphere (temperature range: room temperature to 350 °C). Thermogravimetric analysis (TGA) was conducted with a PerkinElmer TGA 7 equipped with a TGA 7/3 instrument controller at a heating rate of 20 °C/min under nitrogen (temperature range: room temperature to 900 °C). The absolute quantum-yield measurements were carried out using a fluorescence photometer (QuantaMaster Photon Technology International (PTI)) equipped with an integrating sphere.

2.3. Monomer synthesis

2.3.1. Diethyl 2,5-dihydroxyterephthalate (**1**)

To a solution of 2,5-dihydroxyterephthalic acid (5 g, 25 mmol) in 200 mL of ethanol, 13 mL of sulfuric acid was added. The mixture was stirred at 90 °C for 24 h and then cooled to room temperature. The precipitate was filtered and recrystallized from ethanol to afford **1** (5.07 g, 80%) as a greenish needle-like crystal. ^{1}H NMR ($CDCl_3$, ppm): δ 10.05 (s, 2H), 7.46 (s, 2H), 4.32 (q, 4H), 3.96 (t, 6H). ^{13}C NMR ($CDCl_3$, ppm): δ 165.3, 150.8, 120.0, 115.0, 61.1, 13.4.

2.3.2. Diethyl 2,5-bis(hexadecyloxy)terephthalate (**2**)

To a solution of **1** (5 g, 20 mmol) and 1-bromohexadecane (30.6 mL, 100 mmol) in 200 mL of dimethylformamide (DMF) K_2CO_3 (13.6 g, 100 mmol) was added at room temperature. The suspension was stirred at 90 °C for 96 h. After the reaction, the reaction mixture was cooled to room temperature, and the solvent was removed by evaporation under vacuum. The crude product was purified twice by recrystallization from ethanol, affording 12.1 g (89%) of a white powder. ^{1}H NMR ($CDCl_3$, ppm): δ 7.32 (s, 2H), 4.38 (m, 4H), 3.41 (t, 4H), 2.20–1.28 (m, 56H), 0.93 (br, 6H). ^{13}C NMR ($CDCl_3$, ppm): δ 165.8, 148.4, 117.9, 114.7, 68.2, 61.4, 32.9, 28.7, 25.6, 23.0, 14.3.

2.3.3. 2,5-Bis(hexadecyloxy)terephthalohydrazide (**3**)

An 8.8-mL (284 mmol) quantity of hydrazine hydrate was added to a three-necked 500-mL flask containing 100 mL of methanol, and the temperature was raised to 65 °C. A 5-g (7.1 mmol) quantity of **2** dissolved in 200 mL of methanol was slowly added into the mixture with vigorous stirring. The reaction was continued for 24 h. After the reaction, the mixture was evaporated to a volume of 50 mL. The mixture was cooled, and the precipitate was isolated by filtration. The solid was recrystallized twice from ethanol, affording 4.2 g (88%) of a white powder. ^{1}H NMR ($CDCl_3$, ppm): δ 9.2 (s, 2H), 7.8 (s, 2H), 4.2 (t, 4H), 2.2–1.28 (m, 60H), 0.9 (t, 6H). ^{13}C NMR ($CDCl_3$, ppm): δ 164.8, 147.4, 123.2, 112.7, 68.2, 61.4, 31.9, 28.9, 25.6, 23.0, 14.1.

2.3.4. Diethyl 2,5-bis(2-ethylhexyloxy)terephthalate (**4**)

To a solution of **1** (5 g, 20 mmol) and 17.6 mL of 2-ethylhexylbromide (100 mmol) in DMF (200 mL) K_2CO_3 (13.6 g, 100 mmol) was added at room temperature. The suspension was stirred at 90 °C for 96 h. After the reaction, the reaction mixture was cooled to room temperature and the solvent was removed by evaporation under vacuum. The remaining liquid was transferred to a separatory funnel, and ether was added. The mixture was washed with water twice and dried over magnesium sulfate. After the removal of ether under vacuum, **4** was obtained as a yellow liquid (7.8 g, 82%). ^{1}H NMR ($CDCl_3$, ppm): δ 7.33 (s, 2H), 4.39 (m, 4H), 3.91 (t, 4H), 1.82–1.03 (br, 24H), 0.92–0.81 (br, 6H). ^{13}C NMR ($CDCl_3$, ppm): δ 165.8, 149.5, 118.5, 114.7, 75.2, 60.4, 40.3, 30.7, 29.8, 24.7, 22.9, 14.3, 12.1.

2.3.5. 2,5-Bis(2-ethylhexyloxy)terephthalic acid (**5**)

Into a three-necked 250-mL flask containing 100 mL of 30 wt.% KOH aqueous solution, 10 g (20.9 mmol) of **4** was added with vigorous stirring. The reaction mixture was maintained at 100 °C for 24 h. After the reaction, the mixture was cooled to 0 °C and was neutralized with hydrochloric acid to obtain a precipitate. The precipitate was isolated by filtration, purified twice by recrystallization from ethanol, and dried in a vacuum oven yielding 8.2 g (94%). ^{1}H NMR ($CDCl_3$, ppm): δ 12.80 (s, 2H), 7.28 (s, 2H), 4.30

(m, 4H), 3.91 (t, 4H), 1.82–1.03 (br, 24H), 0.92–0.81 (br, 6H). ^{13}C NMR ($CDCl_3$, ppm): δ 169.0, 149.2, 119.7, 115.1, 75.0, 40.5, 30.9, 29.4, 25.1, 23.1, 14.3, 12.1.

*2.3.6. 2,5-Bis(2-ethylhexyloxy)benzene-1,4-dioyl dichloride (**6**)*

A 2.0-g (4.7 mmol) quantity of **5** and three drops of DMF were added to a three-necked 100-mL flask containing 50 mL of thionyl chloride. The suspension was heated to reflux for 24 h. Thionyl chloride was removed under reduced pressure, and the product used without further purification for the next step.

*2.3.7. 1,4-Dihydro-4-oxopyridine-2,6-dicarbonyl dichloride (**7**)*

A 2.5-g (11.5 mmol) quantity of chelidamic acid and 50 mL of distilled thionyl chloride were added into a 3-necked 100 mL flask with three drops of DMF. The suspension was heated to reflux for 24 h. Thionyl chloride was removed under reduced pressure and the product used without further purification for the next step.

2.4. Polymer synthesis

*2.4.1. Precursor polymer (**P1**)*

In a 250-mL flask, 0.7 g (3.0 mmol) of **7** in 13 mL of methylene chloride and 1.4 g (3.0 mmol) of **6** in 17 mL chloroform were added. A 2-mL quantity of triethylamine was added to the mixture with stirring. A 4.0-g (5.9 mmol) quantity of **3** dissolved in 20 mL of chloroform was added slowly, and the reaction was carried out for 2 h. After polymerization, a precipitate was obtained by pouring the mixture into 600 mL of methanol. The polymer was washed twice in water and finally in methanol. The polymer was redissolved in 50 mL of chloroform and precipitated in acetone. A pale

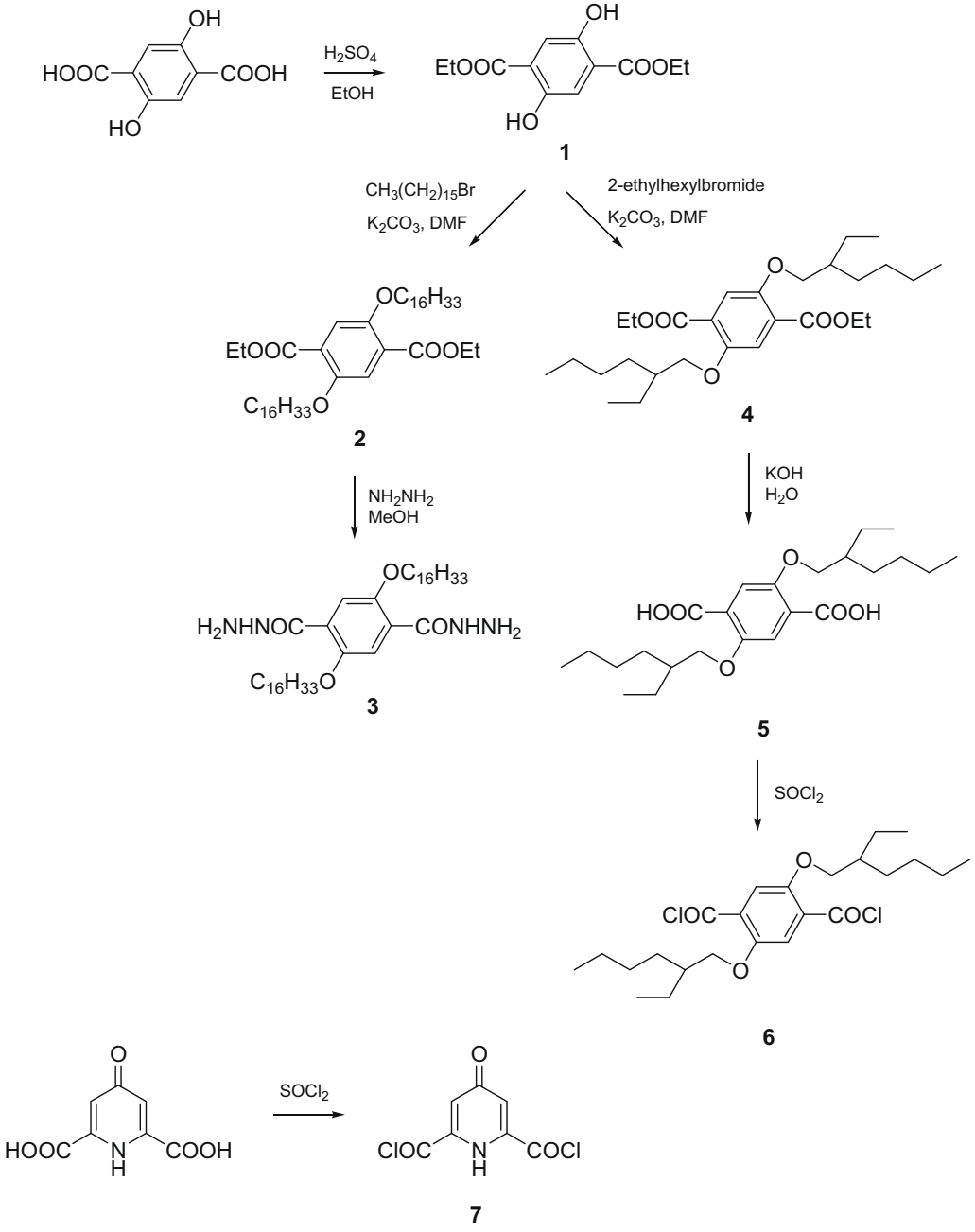

Scheme 1. Synthesis of monomers.

yellowish powder was obtained after drying in a vacuum oven, yielding 3.8 g (67%). ^{1}H NMR ($CDCl_3$, ppm): δ 11.51 (s) 9.17 (s), 7.86 (d), 4.17–4.08 (m), 2.17–1.51 (m). ^{13}C NMR ($CDCl_3$, ppm): δ 207.11, 165.67, 151.23, 123.29, 115.89, 77.65, 77.43, 77.22, 76.80, 72.43, 39.59, 32.13, 31.12, 31.01, 29.91, 29.88, 29.71, 29.57, 29.48, 29.40, 29.29, 29.19, 26.29, 24.44, 23.16, 22.89, 14.31, 14.21, 11.30. Anal. Calcd. (%) for $C_{57.16}H_{96.80}O_{12.37}N_{4.51}$: C, 70.92; H, 10.00; N, 6.54. Found: C, 71.01; H, 11.05; N, 6.73.

*2.4.2. Oxadiazole polymer (**P2**)*

In a 50-mL flask, 0.3 g of **P1** and 10 mL of phosphorous oxychloride were heated to 110 °C for 24 h. The reaction mixture was cooled to room temperature, and then it was poured into 500 mL of ice water. The precipitate was isolated by filtration and washed sequentially with water and acetone. The polymer was redissolved in 50 mL of chloroform and precipitated in 500 mL of acetone. A dark yellowish powder was obtained after drying in a vacuum oven. ^{1}H NMR ($CDCl_3$, ppm): δ 10.51 (s), 8.03–7.63 (m), 4.43–3.87 (m), 2.16–1.39 (m). 13C NMR ($CDCl_3$, ppm): δ 207.11, 166.24, 163.35, 161.03, 156.50, 152.34, 151.03, 124.59, 124.14, 117.03, 73.83, 73.55, 70.30, 70.21, 70.19, 70.13, 69.91, 61.57, 52.49, 39.40, 32.12, 31.10, 29.90, 29.56, 26.11, 25.71, 23.76, 23.21, 22.88, 14.30, 10.82. Anal. Calcd. (%) for $C_{54.89}H_{95.32}O_{5.48}N_{3.87}$: C, 72.78; H, 10.53; N, 5.99. Found: C, 71.02; H, 10.28; N, 5.99.

2.5. Fluorescence patterning

Thin films of **P2** were obtained via spin-casting from a 0.5 wt.% chloroform solution onto a glass slide or a silicon wafer. After drying in vacuo at 50 °C for 12 h, the film was exposed through a photomask to a monochromatic 254 nm UV light with an intensity of 630 μW/cm^2 from a hand-held UV lamp (the distance from the UV lamp to the film was 5 cm). The fluorescent image photographs were taken by a fluorescence microscope equipped with a cooled CCD camera (Meta Imaging Series 4.6, Universal Imaging Corp.).

3. Results and discussion

The synthetic routes for the diacid chlorides **6** and **7** and dihydrazide monomer **3** are shown in Scheme 1. Monomers **3**, **6**, and **7** were prepared with good yields according to previously reported methods with slight modifications [32,33]. The copolyhydrazide **P1** was easily obtained by reactions with **3**, **6**, and **7** in chloroform and methylene chloride. For oxadiazole ring formation, **P1** was reacted in phosphorous oxychloride for 24 h. The copolymer composition of each polymer was calculated from elemental analysis data. It was found that the molar composition (as a mole fraction) x was calculated to be 0.64 in the polymer backbone. The copolyoxadiazole **P2** as well as the precursor copolyhydrazide **P1** showed good solubility in common organic solvents such as chloroform, THF, DMF, and DMSO, but they were not soluble in acetone and methanol. The molar composition (x) was found to be 0.67 from the integral calculation from the ^{1}H NMR spectrum of **P2**. The compositions calculated from the elemental analysis and ^{1}H NMR data were in reasonable agreement. During the polymerization reaction, the pyridone group was converted into a hydroxypyridine unit, with a chemical shift around 10 ppm (for hydroxyl group) in the NMR spectrum similar to the previous reports [33,34]. It is plausible that such a downfield-shifted peak of the hydroxyl group resulted from a weakening of O—H bond in the presence of intermolecular hydrogen bonding.

TGA and DSC were employed to investigate the thermal behaviors of the polymers. As shown in Fig. 1, the onset decomposition temperatures (T_d) of **P1** and **P2** were found to be 398.5 and 415.2 °C, respectively. The onset T_d of **P2** was higher than that of **P1,** as expected, in which the thermally stable oxadiazole unit played a role in its thermal stability. However, the glass-transition temperatures (T_g) of the polymers were not found even in the second scan in the DSC investigation.

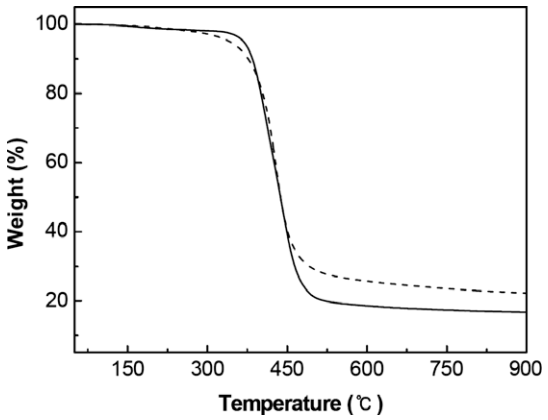

Fig. 1. TGA thermograms of the precursor polymer **P1** (dotted) and **P2** (solid) under a nitrogen atmosphere.

The number-average molecular weights (M_n) of the precursor polymers **P1** and **P2** were measured at 25,350 and 24,210, respectively, according to the GPC analysis. The weight-average molecular weights (M_w) of **P1** and **P2** were found to be 49,710 and 41,410,

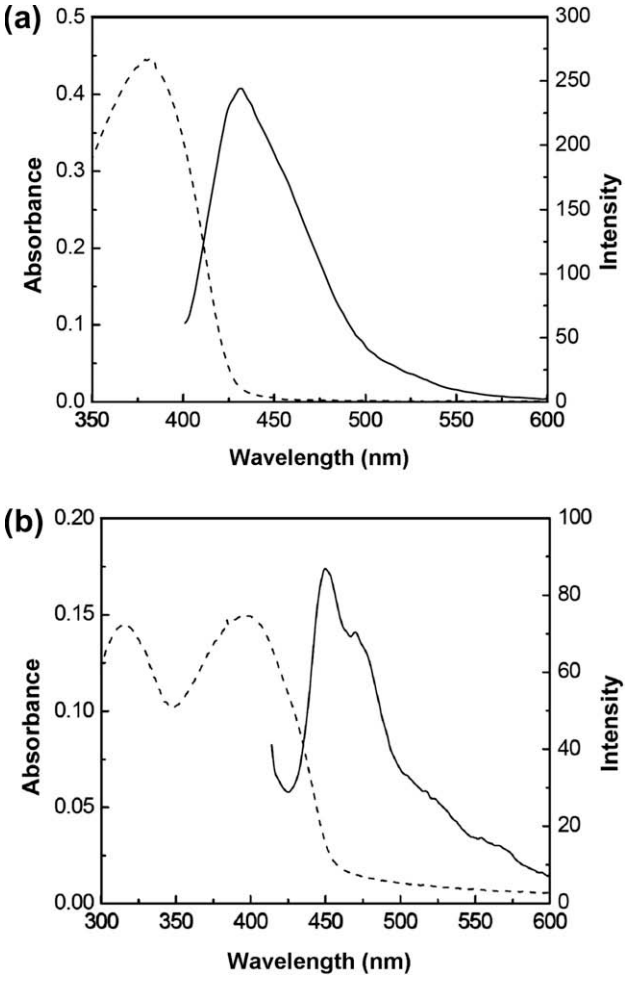

Fig. 2. Absorption (dotted, 9.2 × 10^{-6} M) and emission spectra (solid, 7.4 × 10^{-9} M) of (a) **P2** solution in chloroform and (b) **P2** film.

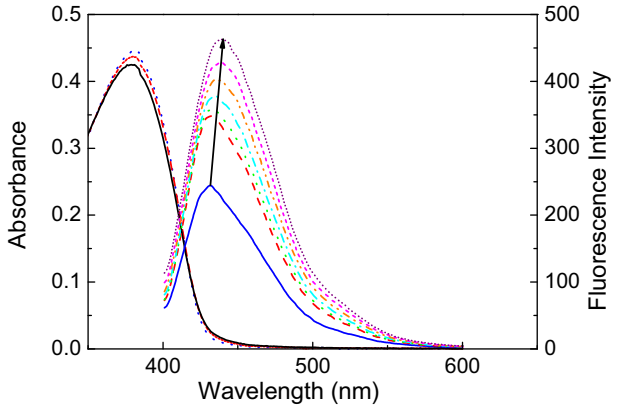

Fig. 3. Absorption (9.2×10^{-6} M) and emission (7.4×10^{-9} M) spectra of the **P2** solution in chloroform upon UV irradiation (time: 0, 15, and 20 min for absorption; 0, 5, 10, 15, 20, 25, and 30 min for emission).

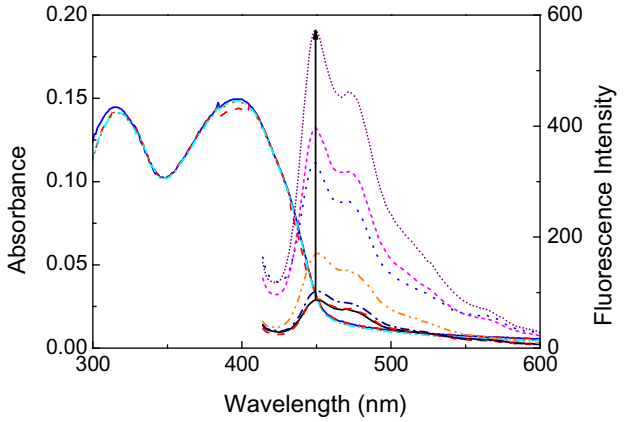

Fig. 4. Absorption and emission spectra of the **P2** film upon UV irradiation (time: 0, 10, 20, and 30 min for absorption; 0, 5, 10, 15, 20, 25, and 30 min for emission).

respectively. The molecular weight difference between **P1** and **P2** is ascribed to the difference in the hydrodynamic volume resulting from the difference in chain flexibility between hydrazide and the oxadiazole ring.

Fig. 2 shows the absorption and emission spectra of **P2** in chloroform solution at the concentrations of 9.2×10^{-6} M and 7.4×10^{-9} M, respectively (Fig. 2a), and in the solid film (Fig. 2b). The absorption maxima of **P2** in the solutions and in the film were located at 382 nm, 314 nm, and 397 nm, respectively. Besides showing a new absorption band at a short wavelength (314 nm), a red shift of the absorption (382 nm to 397 nm) was observed by comparing the λ_{max} values of the solutions and the solid. The photoluminescence of the **P2** film shown in Fig. 2b is different from that of the solution (Fig. 2a) in both emission-band positions and the shapes of the spectra. A large red shift of the emission maximum (about 18 nm) and the formation of a new emission shoulder about 470 nm were shown in the film state. We found that the excitation spectra from the emission at 450 nm and at 470 nm were the same as the absorption spectrum in the solid state. It is presumed that the large red shift in absorption and emission indicates the presence of intermolecular interactions between molecular backbones, which is in accordance with our synthetic strategy [35,36].

In our previous report, we showed that the intermolecular interaction between polymer backbones can be manipulated by UV irradiation, which induced fluorescence quenching at exposed areas of the polymer film [28]. In that system, intermolecular π-interaction played a crucial role in fluorescence manipulation. In

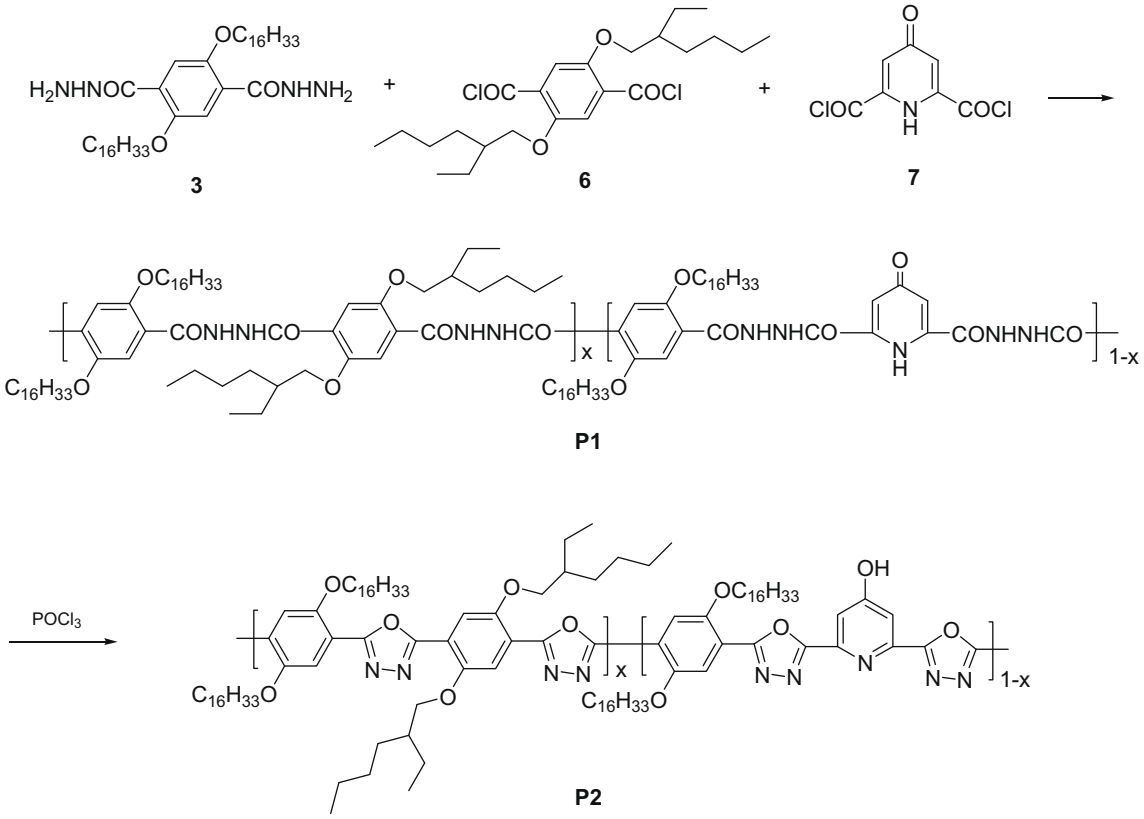

Scheme 2. Synthesis of polymer.

contrast to such a fluorescence-quenching system, the fluorescence intensity of the **P2** solution was greatly enhanced as UV irradiation time increased (more than twofold), as shown in Fig. 3. Considering that there was a negligible change in UV absorption during UV irradiation, possible chemical degradation or photobleaching by UV irradiation was not expected; the photochemically stable oxadiazole ring might have provided this advantage [18]. With UV irradiation, a gradual increase in fluorescence intensity as well as slight red shift of the emission maximum (from 432 nm to 439 nm) was observed, as shown in Fig. 3, indicative of the possible photo-oxidation of the hydroxypyridine ring to form a keto tautomer such as a pyridone ring [37,38].

This unique phenomenon regarding the fluorescence enhancement by UV irradiation was also observed in the film state, as shown in Fig. 4. Similarly to the case of the solution, UV absorption did not change upon UV irradiation even after a prolonged time. In a manner similar to the **P2** solution, the **P2** film exhibited fluorescence enhancement upon UV illumination, which was likely due to the same photo-oxidation mechanism to form the keto tautomer [39]. The degree of fluorescence intensity increase was proportional to the UV irradiation time without emission-maximum change. Although there was no shift in absorption and emission, we believe that the much larger fluorescence enhancement in the **P2** film compared to that of the solution resulted from the facilitated photochemical conversion of 4-hydroxypyridine groups to 4-pyridone groups that may have been influenced by the closer proximity of the molecular chains in the solid.

We measured the absolute quantum yields of **P2** in solution and in the solid state to test for possible photochemical degradation. The fluorescence quantum yields of **P2** in chloroform solution (4.21×10^{-6} M) and in a thin film were 35% and 0.95%, respectively. The thin film was exposed to UV irradiation to enhance the fluorescence up to 3.5%. The irradiated polymer film was redissolved in chloroform for quantum-yield measurement. The fluorescence quantum yield of the solution recovered to 32%, close to that of the pristine polymer solution. This recovery of quantum yield strongly indicates that there was no new formation of small fluorescent molecular species by photochemical degradation.

We carried out the same experiment of UV irradiation on the film of a polymer (**P3**), i.e., $x = 1$ in **P2** in Scheme 2.

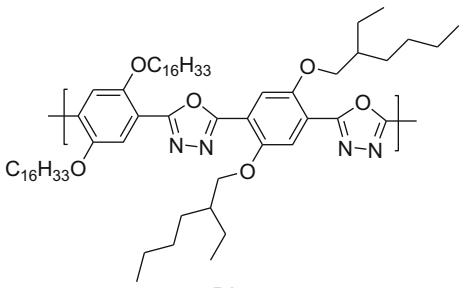

P3

The fluorescence intensity of the **P3** film was not changed by UV irradiation. Thus, it can be concluded that the photosensitized hydroxypyridine units were essential for the photo-induced fluorescence enhancement in this system. We employed spectroscopic methods such as IR, NMR and X-ray photoelectron spectroscopy (XPS) to investigate the structural changes in **P2** before and after UV irradiation; unfortunately, we were not able to determine any differences in their chemical structures due to irradiation. It is likely that the fluorescence-enhancement phenomenon upon UV irradiation is related to the conversion of the hydroxypyridine unit to a pyridone group upon photoirradiation, as has been reported previously [29–31].

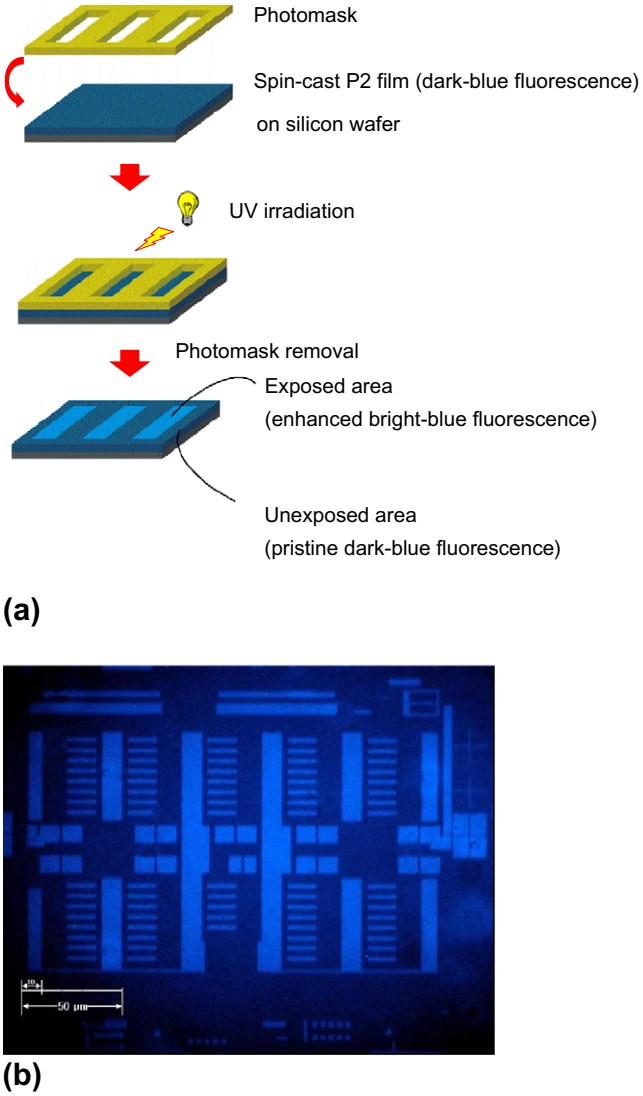

Fig. 5. (a) Schematic diagram of the fluorescent patterning process and (b) fluorescence patterned image through a photomask on a silicon wafer by UV irradiation for 30 min. The polymer film was spin-cast from 0.5 wt.% chloroform solution without PAG. The bright blue fluorescent region was exposed to UV. (For interpretation of the references to colour in this figure legend, the reader is referred to the web version of this article.)

Finally, latent fluorescence images were fabricated in a spin-cast film of **P2** in the absence of PAG by simple irradiation from a 254 nm hand-held UV lamp through a photomask for 30 min, for which the process is illustrated in Fig. 5a. As shown in Fig. 5b, the irradiated **P2** film was highly emissive, with a bright blue fluorescence. The dark blue fluorescent image was made on the unexposed area through the photomask. Fine patterning could be accomplished, with an emissive line width as low as 1 μm depending onto the photomask used. Latent patterns could not be observed under ambient light, while highly resolved fluorescence patterns were clearly seen under UV light. The patterned image was stable for more than a month, maintaining its enhanced fluorescence intensity and resolution at ambient conditions. After that time, the intensity decreased gradually for about a month.

4. Conclusions

We have synthesized a new conjugated polymer containing hydroxypyridine groups linked with oxadiazole units for the

purpose of introducing the combination of facile photosensitization (hydroxypyridine) with thermal and photochemical stability (oxadiazole). Both the polymer solution and the film showed fluorescence enhancement upon UV irradiation, likely due to the conversion of hydroxypyridine to pyridone groups, which influenced the intermolecular interactions between polymer backbones. The initial weak fluorescence intensity could be recovered by redissolving the polymer film with enhanced fluorescence, suggesting that the fluorescence enhancement was not due to a photochemical degradation by UV irradiation. By exploiting the unique optical characteristics of this system, we prepared a novel example of fluorescence imaging of a fluorescence pattern with enhanced intensity by simple UV irradiation.

Acknowledgments

Financial support from the Korea Science and Engineering Foundation (KOSEF) funded by the Korea Government (MEST) is gratefully acknowledged (No. R01-2007-000-10740-0 and 2009-008146).

References

[1] G. Hadziioannou, P.F. van Hutten (Eds.), Semiconducting Polymers, Wiley-VCH, Weinheim, 2000.
[2] T.A. Skotheim, R.L. Elsenbaumer, J. Reynolds (Eds.), Handbook of Conducting Polymers, second ed., Marcel Dekker, New York, 1997.
[3] P. Chandrasekhar, Conducting Polymers: Fundamentals and Applications, Kluwer, Boston, 1999.
[4] S. Miyata, H.S. Nalwa (Eds.), Organic Electroluminescence Materials and Devices, Gordon and Breach, Amsterdam, 1997.
[5] D.T. McQuade, A.E. Pullen, T.M. Swager, Chem. Rev. 100 (2000) 2537.
[6] A.J. Heeger, Angew. Chem. Int. Ed. Engl. 40 (2001) 2591.
[7] G. Yu, J. Gao, J.C. Hummelen, F. Wudl, A.J. Heeger, Science 270 (1995) 1789.
[8] D.L. Wise, G.E. Wnek, D.J. Trantolo, T.M. Cooper, J.D. Gresser, Photonic Polymer Systems, Marcel Dekker, New York, 1998.
[9] H.J. Kim, J.H. Lee, M. Lee, T.S. Lee, React. Funct. Polym. 68 (2008) 1696.
[10] Q. Fang, T. Yamamoto, J. Polym. Sci., Part A: Polym. Chem. 42 (2004) 2686.
[11] T.H. Kim, H.J. Kim, C.G. Kwak, W.H. Park, T.S. Lee, J. Polym. Sci., Part A: Polym. Chem. 44 (2006) 2059.
[12] B. Schulz, M. Bruma, L. Brehmer, Adv. Mater. 9 (1997) 601.
[13] C.K. Kwak, C.-H. Lee, T.S. Lee, Tetrahedron Lett. 48 (2007) 7788.
[14] Y. Yang, Q. Pei, J. Appl. Phys. 77 (1995) 4807.
[15] B. Xu, Y. Pan, J. Zhang, Z. Peng, Synth. Met. 114 (2000) 337.
[16] Y. Chen, C.-K. Liao, T.-Y. Wu, Polymer 43 (2002) 4545.
[17] O. Bolton, J. Kim, J. Mater. Chem. 17 (2007) 1981.
[18] K. Lee, H.-J. Kim, J.C. Cho, J. Kim, Macromolecules 40 (2007) 6457.
[19] J.-M. Kim, Macromol. Rapid Commun. 28 (2007) 1191 (and references therein).
[20] L. Zhao, Z. Lei, X. Li, S. Li, J. Xu, B. Peng, Chem. Phys. Lett. 420 (2006) 480.
[21] J.-M. Kim, J.-H. Kang, D.-K. Han, C.-W. Lee, K.-D. Ahn, Chem. Mater. 10 (1998) 2332.
[22] M. Frenette, C. Coenjarts, J.C. Scaiano, Macromol. Rapid Commun. 25 (2004) 1628.
[23] K.-M. Kim, S.J. Min, S.W. Lee, J.H. Bok, J.S. Kim, Chem. Commun. (2005) 3427.
[24] J. Ohshita, T. Uemura, D.-H. Kim, A. Kunai, Y. Kunugi, M. Kakimoto, Macromolecules 38 (2005) 730.
[25] H.J. Kim, J.H. Lee, C.K. Kwak, W.K. Son, W.H. Park, T.S. Lee, Text. Sci. Technol. 43 (2006) 228.
[26] M.S. Choi, J.H. Lee, D.W. Kim, T.S. Lee, J. Polym. Sci., Part A: Polym. Chem. 45 (2007) 4430.
[27] M.S. Choi, H.J. Kim, W.S. Lyoo, T.S. Lee, High Perform. Polym. 19 (2007) 531.
[28] J.K. Lee, H.-J. Kim, T.H. Kim, C.-H. Lee, W.H. Park, J. Kim, T.S. Lee, Macromolecules 38 (2005) 9427.
[29] J.H. Boyer, S. Kruger, J. Am. Chem. Soc. 79 (1957) 3552.
[30] N.L. Sakina, A.M. Golubkov, L.D. Smirmov, M.A. Ostrovsky, A.E. Dontsov, Bull. Exp. Biol. Med. 147 (2009) 193.
[31] G.T. Wondrak, M.J. Roberts, M.K. Jacobson, E.L. Jacobson, J. Biol. Chem. 279 (2004) 30009.
[32] Z.-Q. Wu, X.-K. Jiang, S.-Z. Zhu, Z.-T. Li, Org. Lett. 6 (2004) 229.
[33] T. Hirao, T. Moriuchi, T. Ishikawa, K. Nishimura, S. Mikami, Y. Ohshiro, I. Ikeda, J. Mol. Catal. A: Chem. 113 (1996) 117.
[34] T.D. Dang, N. Venkatasubramanian, E.W. Baum, W.A. Feld, F.E. Arnold, PMSE Prepr. (Div. Polym. Mater.: Sci. Eng., ACS) 84 (2001) 467.
[35] H. Fukumoto, T. Yamamoto, J. Polym. Sci., Part A: Polym. Chem. 46 (2008) 2975.
[36] C.-F. Liao, B.-Y. Hsieh, Y. Chen, J. Polym. Sci., Part A: Polym. Chem. 47 (2009) 149.
[37] S.P. Bag, Q. Fernando, H. Freiser, Inorg. Chem. 1 (1962) 887.
[38] M. Ignatova, M. Sepulchre, N. Manolova, Eur. Polym. J. 38 (2002) 33.
[39] D.W. Brousmiche, A.G. Briggs, P. Wan, Photochemistry of hydroxyaromatic compounds, in: V. Ramamurthy, K.S. Schanze (Eds.), Organic, Physical, and Materials Photochemistry, Marcel Dekker, New York, 2000, pp. 1–32.